

CFD Analysis of Effect of Variation in Angle of Attack over NACA 2412 Airfoil through the Shear Stress Transport Turbulence Model

Shivananda Sarkar¹ Shaheen Beg Mughal²

¹M.Tech Student ²Assistant Professor

^{1,2}Department of Mechanical Engineering

^{1,2}School of Engineering & Technology, ITM University, Gwalior

Abstract— Airfoil is the shape of a wing, which plays a pivotal role in generating adequate lift to adjust the heaviness of the aircraft body and to help it fly. Simulation for NACA 2412 airfoil was performed using the available Computational Fluid Dynamics techniques. The model of the NACA 2412 airfoil was prepared using the coordinates obtained from the University of Illinois' airfoil database. Popular CAE software Ansys (CFX) was used in this case. Firstly, the coordinates were imported to Ansys geometry modeler, and then CFX (Fluid Flow) was used to generate mesh and conduct the experimentation. At the end of model & mesh generation, simulation was done to observe the effect of flow on the said airfoil model at a high Reynolds number and the variation in angle of attack with respect to the aerodynamic forces acting on it. To conduct the entire experiment, I did not opt for physical set up as the physical model has to be placed inside a wind tunnel, and this process is quite laborious, time consuming and expensive too at the same time. Moreover, the wind tunnel experiments are subjected to the accuracy of the developed model. With the advancement of high configured computers and computational methods, the flow behaviors of the fluid and its effect can be accurately analyzed.

Key words: CFD, The Shear Stress Transport Turbulence Model

I. INTRODUCTION

The study and understanding of aerodynamic flows and their interactions with structures are becoming increasingly important and necessary for aeronautical vehicles. The NACA airfoils are airfoil shapes for aircraft wings developed by the National Advisory Committee for Aeronautics. NACA 2412 is a four-digit airfoil series which possesses a cord length of 1 meter. The lift on an airfoil is primarily the result of its angle of attack and shape. Any object with an angle of attack in a moving fluid, such as a flat plate, a building, or the deck of a bridge, will generate an aerodynamic force (called lift) perpendicular to the flow. When oriented at a suitable angle, the airfoil deflects the oncoming air (for fixed-wing aircraft, a downward force), resulting in a force on the airfoil in the direction opposite to the deflection. Airfoil design is a major facet of aerodynamics. Various airfoils serve different flight regimes. Asymmetric airfoils can generate lift at zero angle of attack, while a symmetric airfoil may better suit frequent inverted flights as in an aerobatic plane. Supersonic airfoils are much more angular in shape and can have a very sharp leading edge, which is very sensitive to angle of attack. A supercritical airfoil has its maximum thickness close to the leading edge to have a lot of length to slowly shock the supersonic flow back to subsonic speeds.

A. Nomenclature of Airfoil

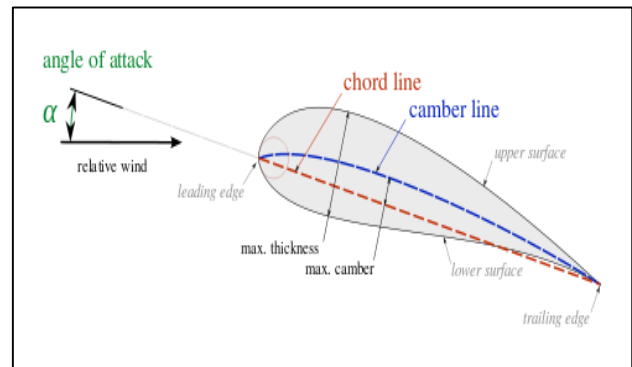


Fig. 1: Airfoil Nomenclature

- The chord line is the connection line between leading and trailing edge and it is straight.
- The chord length is the length of the chord line.
- Angle of attack is defined as the angle between the chord line and relative wind.
- The leading edge is the front point of an airfoil where we get maximum curvature chord. It is the length of the chord line.
- The trailing edge is the part of an airfoil where we find maximum curvature.
- Total aerodynamic force (TAF) is the total force on the airfoil produced by the airfoil shape and relative wind.
- Lift is the perpendicular component of TAF to the relative wind or flight path.
- Drag is the parallel component of TAF to the relative wind or flight path.
- Camber – maximum distance between the mean camber line and the chord line, measured perpendicular to the chord.
- Maximum thickness is the maximum separation from the bottom edge to the top edge. It is generally 0.12c or 12% of the chord
- Maximum camber is the maximal distance of the maximum camber line from the chord line.

II. PROBLEM DEFINITION & RESEARCH GOAL

In this work, the focus is on the analysis of flow leading to drag and lift over the NACA Airfoil 2412 model at various angles of attack. When the boundary layer is turbulent, the flow is more resistant to separation, and more lift can be generated due to a delayed stall. A high Reynolds number, 4.5220E+06 is taken for this experiment. The goals of this research are - utilization of computational fluid dynamics with Menter's shear stress transport turbulence model to thorough study and analyze the effect of turbulent flow over NACA 2412, a four digit-series airfoil model, and to obtain the pressure distribution, lift and drag forces at various

angles to determine its optimum angle of attack for maximum efficiency.

III. SST TURBULENCE MODEL

Turbulence modeling is the construction and use of a model to predict the effects of turbulence in the study of CFD. A turbulent fluid flow has features on many different length scales, which all interact with each other. A common approach is to average the governing equations of the flow, in order to focus on large-scale and non-fluctuating features of the flow. However, the effects of the small scales and fluctuating parts must be modelled. One of the most effective is the Shear Stress Transport (SST) model of Menter. The model works by solving a turbulence/frequency-based model ($k-\omega$) at the wall and $k-\epsilon$ in the bulk flow. A blending function ensures a smooth transition between the two models. The SST model performance has been studied in a large number of cases. In a NASA Technical Memorandum, SST was rated the most accurate model for aerodynamic applications. Mathematical equations & formulations of the SST model are shown below

$$\frac{\partial(\rho k)}{\partial t} + \frac{\partial(\rho u_j k)}{\partial x_j} = \rho P - \beta^* \rho \omega k + \frac{\partial}{\partial x_j} \left[(\mu + \sigma_k \mu_t) \frac{\partial k}{\partial x_j} \right]$$

$$\frac{\partial(\rho \omega)}{\partial t} + \frac{\partial(\rho u_j \omega)}{\partial x_j} = \frac{\gamma}{\nu_t} P - \beta \rho \omega^2 + \frac{\partial}{\partial x_j} \left[(\mu + \sigma_\omega \mu_t) \frac{\partial \omega}{\partial x_j} \right]$$

$$+ 2(1 - F_1) \frac{\rho \sigma_{\omega 2}}{\omega} \frac{\partial k}{\partial x_j} \frac{\partial \omega}{\partial x_j}$$

A. Variable Definition:

$$P = \tau_{ij} \frac{\partial u_i}{\partial x_j}$$

$$\tau_{ij} = \mu_t \left(2s_{ij} - \frac{2}{3} \frac{\partial u_k}{\partial x_k} \delta_{ij} \right) - \frac{2}{3} \rho k \delta_{ij}$$

$$s_{ij} = \frac{1}{2} \left(\frac{\partial u_i}{\partial x_j} + \frac{\partial u_j}{\partial x_i} \right)$$

$$\mu_t = \frac{\rho a_1 k}{\max(a_1 \omega, F_2)}$$

$$\phi = F_1 \phi + (1 - F_1) \phi_2$$

$$F_1 = \tanh \left(\arg g_1^4 \right)$$

$$\arg g_1 = \min \left[\max \left(\frac{\sqrt{k}}{\beta^* \omega d}, \frac{500 \nu}{\partial} \frac{\partial^2 \omega}{\partial^2 \omega} \right), \frac{4 \rho \sigma_{\omega 2} k}{CD_{k\omega} d^2} \right]$$

$$CD_{k\omega} = \max \left(2 \rho \sigma_{\omega 2} \frac{1}{\omega} \frac{\partial k}{\partial x_j} \frac{\partial \omega}{\partial x_j}, 10^{-20} \right)$$

$$F_2 = \tanh \left(\arg g_2^2 \right)$$

$$\arg g_2 = \max \left(2 \frac{\sqrt{K}}{\beta^* \omega d}, \frac{500 \nu}{d^2 \omega} \right)$$

B. Constant

$K - W$ Closure: $\sigma_{k1} = 0.85, \sigma_{\omega 1} = 0.65, \beta_1 = 0.075$
 $K - \epsilon$ Closure: $\sigma_{k2} = 1.00, \sigma_{\omega 2} = 0.856, \beta_2 = 0.0828$
 SST Closure Constants: $\beta^* = 0.09 \alpha_1 = 0.31$

C. Far Field Conditions:

$$\frac{U_\infty}{L} < \omega_{farfield} < 10 \frac{U_\infty}{L}$$

$$10^{-5} U_\infty^2 < k_{farfield} < \frac{0.1 U_\infty^2}{R_{eL}}$$

$$\frac{U_\infty}{R_{eL}} < k_{farfield} < \frac{U_\infty}{R_{eL}}$$

Boundary/Wall Conditions

$$\omega_{wall} = 10 \frac{6\nu}{\beta_1 (\Delta d_1)^2}, \quad k_{wall} = 0$$

IV. COMPUTATIONAL MODEL & MESH GENERATION

NACA has developed various models of airfoils. And the co-ordinates of the airfoils can be obtained from the airfoil database of University of Illinois.

Using the Geometry Modeler of Ansys, the imported coordinates were processed to prepare the model. Contour is also generated in the process to conduct the simulation.

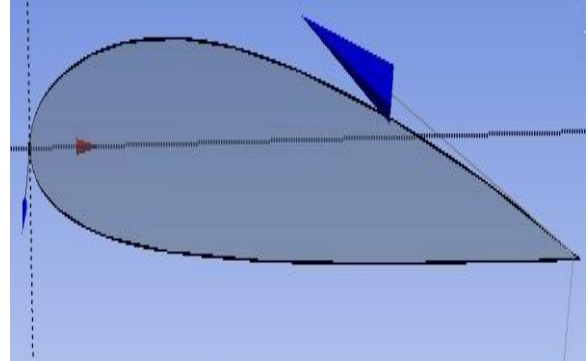


Fig. 2: Geometry of the NACA 2412 Airfoil Model

Mesh generation is the practice of generating a polygonal or polyhedral mesh that approximates a geometric domain. Typical uses are for rendering to a computer screen or for physical simulation such as finite element analysis (FEA) or computational fluid dynamics (CFD).

For the analysis of the flow of fluid, the domains are needed to split into smaller sub domains and mesh accuracy of the domain increases as we go towards the airfoil shape. The governing equations are then discretized and solved inside each of these sub domains. The generated portion of mesh around the airfoil is shown in the figure below

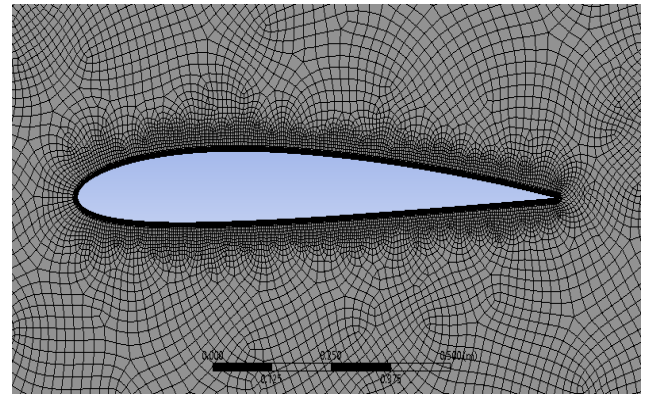


Fig. 3: Mesh generation using Ansys

V. DEFINING THE BOUNDARY CONDITIONS

The most integral part of any CFD problem is the definition of its boundary conditions. The problem for the said airfoil model considers turbulent flow around the airfoil from 0° to 10° angle of attack. To conduct the simulation, boundary conditions for the problem and some initial inputs are taken, and it is shown in the table below-

Sl no	Input	Value
1	Analysis Type	Steady State
2	Fluid Velocity	5.0000E+01 m/s

3	Operating Temperature	25° C
4	Operating Pressure	101325 Pa
5	Fluid Density	1.1850E+00
6	Turbulence Model	SST
7	Reynolds Number	4.5220E+06
8	Dynamic Viscosity	4.9907E+01
9	Angle of Attack	0° - 10°
10	Chord Length	1 m

Table 1:

VI. SIMULATION RESULTS & DISCUSSION

A. Contours of Pressure

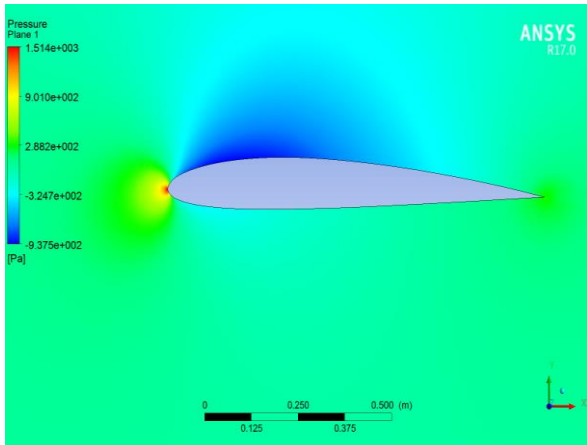


Fig. 4: Pressure contour at 1° AoA

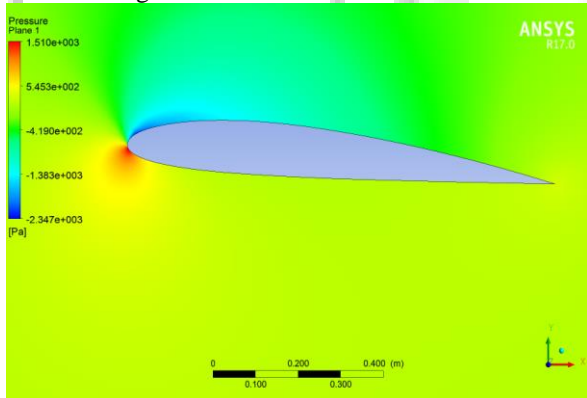


Fig. 5: Pressure contour at 5° AoA

For different angles of attack, the maximum and minimum values of the pressure are of the following order -

AoA	Pressure [Pa]	
	Maximum	Minimum
0°	1.518e+003	-7.971e+002
1°	1.514e+003	-9.375e+002
2°	1.512e+003	-1.117e+003
3°	1.496e+003	-1.373e+003
4°	1.520e+003	-1.831e+003
5°	1.510e+003	-2.347e+003
6°	1.505e+003	-2.889e+003
7°	1.497e+003	-3.493e+003
8°	1.499e+003	-4.213e+003
9°	1.499e+003	-5.175e+003
10°	1.491e+003	-6.312e+003

Table 2:

B. Contours of X Velocity

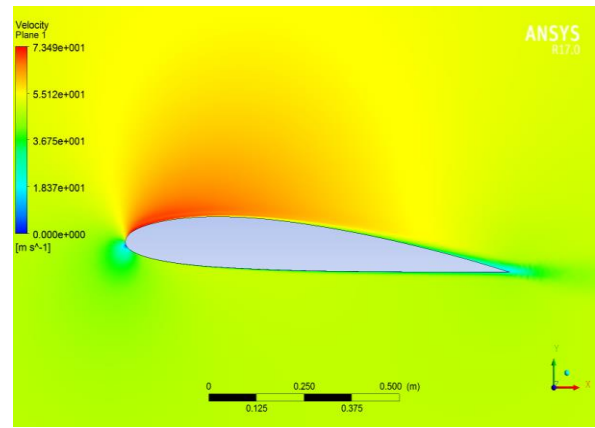


Fig. 6: Velocity contour at 4° AoA

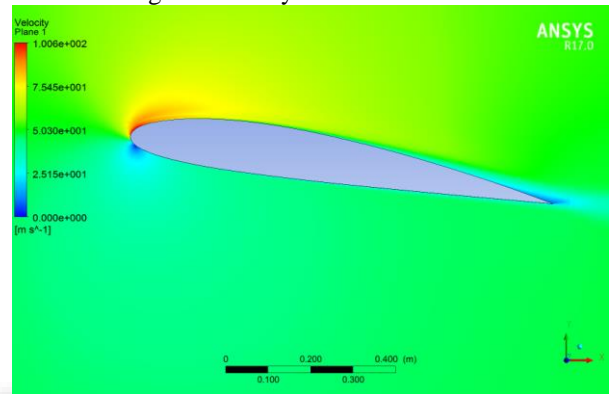


Fig. 7: Velocity contour at 9° AoA

For different angles of attack, the values of the X-velocity are of the following order -

Angle of Attack	Velocity [m/s]
0°	6.207e+001
1°	6.389e+001
2°	6.625e+001
3°	6.880e+001
4°	7.349e+001
5°	7.873e+001
6°	8.389e+001
7°	8.928e+001
8°	9.474e+001
9°	1.006e+002
10°	1.074e+002

Table 3:

C. Contours of Force

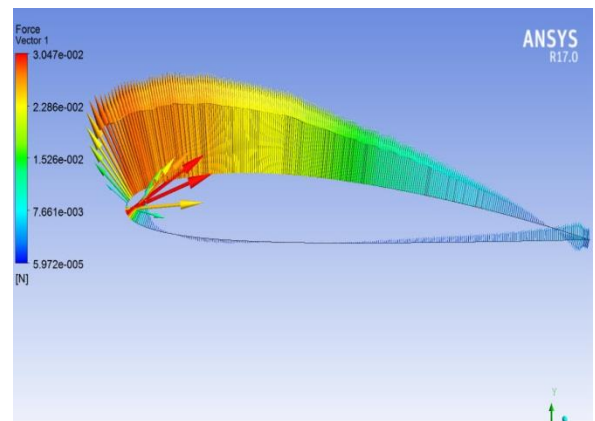


Fig. 8: Total Aerodynamic Force at 3° AoA

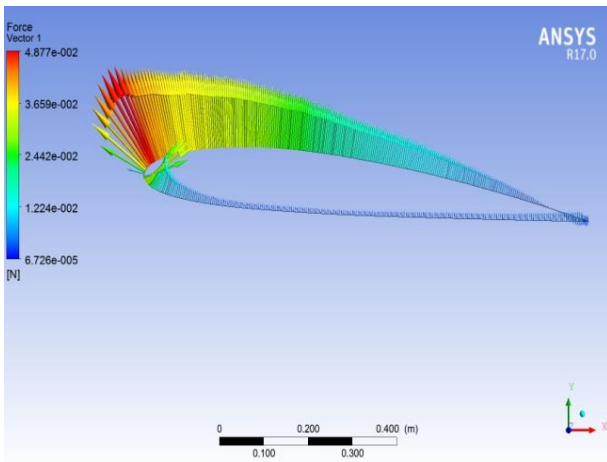


Fig. 9: Total Aerodynamic Force at 5° AoA

A total aerodynamic force is generated when a stream of air flows around an airfoil that is moving through the air.

For different angles of attack, the maximum and minimum values of total aerodynamics force are of the following order -

AoA	Total Aerodynamic Force [N]	
	Maximum	Minimum
0°	3.026e-002	7.412e-005
1°	3.000e-002	7.566e-005
2°	3.059e-002	9.781e-005
3°	3.047e-002	5.972e-005
4°	3.799e-002	8.035e-005
5°	4.877e-002	6.726e-005
6°	5.998e-002	7.428e-005
7°	7.247e-002	1.210e-005
8°	8.734e-002	1.056e-004
9°	1.072e-001	1.056e-004
10°	1.301e-001	2.952e-005

Table 4:

Angle of Attack	Lift Force [N]	Drag Force [N]	Ratio
0°	3.18655	0.153374	20.77634
1°	4.73808	0.164	28.89073
2°	6.26266	0.180278	34.73869
3°	7.78753	0.200345	38.87060
4°	9.30648	0.226209	41.14107
5°	10.8285	0.257091	42.11932
6°	12.2827	0.292499	41.99228
7°	13.7836	0.328802	41.92067
8°	15.1126	0.379664	39.80520
9°	16.4894	0.430878	38.26930
10°	17.7536	0.488309	36.35730

Table 5: The values of Lift Force and Drag Force and their ratios are shown below:

The lift to drag ratio is an important parameter in measuring the airfoil performance. When the Lift to Drag ratio is highest at a particular angle, it means that the drag force has very less value and that particular angle provides greater lift force and maximum efficiency.

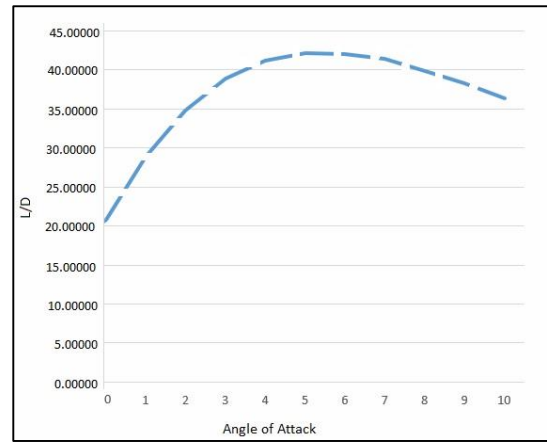


Fig. 10: Lift & Drag Comparison Graph

The L/D chart shows that up to a certain angle, the value of lift to drag ratio increases. The higher the lift to drag ratio, better the efficiency.

VII. CONCLUSION

This research work presents the simulated flow over a NACA 2412 airfoil model at a high Reynolds number with a variation in angle of attack and it has been observed that the lift force and drag force increase respectively as the angle of attack increases. 5° angle of attack has been found to be the optimum angle. At this specific angle, the said airfoil model produces the maximum ratio of Lift & Drag (42.11932), which is ideal for efficient performance compared to other angles of attack. Total Aerodynamics Force for 5° angle of attack is found to be of the order of (N) 4.877e-002 (maximum) and 6.726e-005 (Minimum). And Pressure generated on the airfoil at this specific angle is of the order of (N) 1.510e+003 (maximum), and -2.347e+003 (minimum). 6° and 7° angles are also found to be near optimized with increased lift for sufficient efficiency, but with this, drag force also tends to increase. Therefore, it can be concluded that 5° angle of attack is optimum for the NACA 2412 airfoil model as per the Shear Stress Transport Turbulence Model.

VIII. ACKNOWLEDGEMENT

I would like to express my sincere gratitude to my guide, Assistant Professor, Shaheen Beg Mughal for providing me the opportunity to work with him and his continuous assistance throughout the course of this research work. His constant advice, appreciation and assessment have been vital to me. For me, he has been the pillar of strength all this time. At last, I thank my parents who gave me an upbringing to carry on this work.

REFERENCES

- [1] Theory of Wing Sections: Including a Summary of Airfoil Data by Albert Edward Von Doenhoff and Ira H. Abbott
- [2] Fundamentals of Aerodynamics by Cram textbook reviews, 5th Edition
- [3] http://m-selig.ae.illinois.edu/ads/coord_database.html (Accessed on 4th February)
- [4] <https://turbmodels.larc.nasa.gov/sst.html>. (Accessed on 5 Feb, 2017)

- [5] Gatski T.B., Hussaini M.Y., Lumley, J.L., "Simulation and Modelling of Turbulent Flows, Vol. 1, Oxford Press, 1996
- [6] <https://www.cfd-online.com/> (Accessed on 15 Feb, 2017).

